Turk J Elec Engin, VOL.11, NO.2 2003, © TÜBİTAK

MUSIC, CBF and Differential Algebraic Constant Modulus Algorithms for Direction of Arrival Estimation in Passive Coherent Locators

Ahmet ÖZÇETİN
Hava Kuvvetleri Komutanlığı, Bakanlıklar, Ankara-TURKEY
Ahmet.Ozcetin@ieee.org

Abstract

In passive coherent locators (PCL) systems, noise and the precision of direction of arrival (DOA) estimation are key issues. This paper addresses the implementation of high-resolution DOA estimation methods, in particular the multiple signal classification (MUSIC) algorithm, the conventional beam forming (CBF) algorithm, and the algebraic constant modulus algorithm (ACMA). The goal is to compare the ACMA to the MUSIC and CBF algorithms for application to PCL.

The results and analysis presented here support the use of constant modulus information, where available, as an important addition to DOA estimation. The ACMA offers many simple solutions to noise and separation related problems; at low signal-to-noise ratio levels, it provides much more accurate estimates and yields reasonable separation performance even in the presence of challenging signals. Differential ACMA, which allows the simple digital removal of the direct signal component from the output of a sensor array, is also introduced.

Key Words: *Passive Radar, Direction of Arrival (DOA), Passive Coherent Locators (PCL), Blind Source Separation, Array Antenna, Conventional Beamforming (CBF), Multiple Signal Classification (MUSIC), Differential, Algebraic Constant Modulus Algorithm (ACMA)*

1. Introduction

Radar has been studied for more than a century and will continue to be studied. Even though new techniques have been invented, there is a clear need to find new ways of implementing old techniques, such as passive coherent locators (PCL).

PCL systems are a form of radar that exploit the ambient radiation in the environment to detect, track and identify objects. PCL systems differ from conventional radars in many ways; mainly, they do not radiate energy. Since both the amplitude and phase of the received signal are measured and processed, PCL is a coherent operation. Bistatic radar object parameter measurements, such as range, Doppler, and direction-of-arrival (DOA), can also be applied to PCL. Multistatic measurements, such as time difference of arrival (TDOA) and differential Doppler (DD), are used together with bistatic measurements. PCL uses an emitter of opportunity; therefore, the waveform is constrained to whatever is offered by the non-cooperative

transmitter. The location of the receiver is limited to areas of co-illumination and reception. To determine the location, bearing, and velocity of an object, the receivers will typically use state-of-the-art computing technology to exploit high-resolution signal processing and estimation algorithms. PCL technologies and systems are only now becoming serious candidates for operational use because PCL systems need robust digital processing techniques.

2. Problem

One of the key issues in PCL systems is noise. Harmonics from the transmitter(s) of opportunity, galactic noise, interference from other transmitters within line-of-sight, and multipath, especially due to ground effect, degrade PCL system performance. Thus, thermal noise-limited detection ranges are significantly decreased. Direct source signal, or reference source signal at the receiving antenna, also causes problems in detection and DOA estimation. A DOA estimation algorithm, which is able to bias out noise to some degree and remove the direct source signal component from the antenna output, is very helpful in increasing detection ranges.

Another problem lies in the precision of DOA estimation. In a two-element interferometer system, the difficulties of accurately estimating phase at low signal-to-noise ratio(s) (SNR), and the effects of multipath propagation cause large error variance in DOA profiles. The DOA change rate is slower for objects at longer ranges than for objects at closer ranges, and the small changes in DOA will be swamped by noise. These problems result in insufficient information in Doppler and DOA profiles, which with typical measurement errors will degrade the accuracy of the object state estimate [1]. Thus, a high-resolution DOA estimation algorithm is a necessity.

A two-element interferometer is the simplest and cheapest means of direction finding. If more channels are available, then additional sensors can be arranged in an array, and then other direction finding techniques such as conventional beamforming, adaptive beamforming and super-resolution can be used. This will give better performance at the expense of complexity.

3. Summary of Current Knowledge

There are several methods of finding DOA, such as by interferometer, Doppler, differential Doppler, TDOA, etc. Griffiths and Long [2], and Howland [1] used phase interferometry for DOA measurements with two simple Yagi antennas. They had difficulties for DOA measurements with off-boresite signals.

Howland used the Cramèr-Rao lower bound (CRLB) to quantify the performance of the system. In his system, Howland managed to detect almost all objects seen by secondary surveillance radar (SSR), but tracked only one-third of them. Howland concluded that objects might be lost in CFAR or Kalman filtering or by having ambiguous or too inaccurate bearing estimates [1].

The silent Sentry® system uses a horizontal linear phased array antenna to collect object echo. The system integrates FM and TV tracks by extracting the TDOA and Doppler measurements for each detected object by using beamforming techniques [3]. It combines sophisticated signal processing techniques with up-to-date radar achievements.

Beamforming techniques try to separate the super-positions of source signals from the outputs of a sensor array. "The objective of blind beamforming is to do this without training information, relying instead on various structural properties of the problem" [4]. DOA estimation methods exploit either the parametric

structure of the array manifold or properties of the signals such as being non-Gaussian, or cyclo-stationary. In these kinds of methods, the signal waveform estimation is done by multiplying a weight matrix by the received data matrix. A well-studied example of the first type is the estimation of signal parameters via the rotation invariance technique (ESPRIT) algorithm, which is based on a constant delay and attenuation between any two adjacent samples in a uniformly sampled time and space series [5]. A representative of the second type is the algebraic constant modulus algorithm (ACMA), which gives algebraic expressions for the separation of sources based on their constant modulus property, valid for phase-modulated sources. Van Der Veen showed that the two properties could be combined into a single algorithm [4].

Leshem introduced a Newton scoring algorithm for the maximum likelihood separation and DOA estimation of constant modulus signals, using a calibrated array. "The main technical step is the inversion of the Fisher information matrix, and an analytic formula for the update step in the Newton method, based on initialization with a sub-optimal method" [6]. Leshem presented the computational complexity of the algorithm and demonstrated its effectiveness by simulations.

Trump and Ottersten analyzed least square based algorithms and proposed a weighted least square algorithm. They proved the asymptotic efficiency of the proposed algorithm and provided the CRLB [7].

ACMA offers solutions for problems related with noise level and DOA resolution; however, it has never been used in PCL systems before. This work combines the current knowledge about digital beamforming techniques and PCL.

4. Scope

The goal of this study is to compare the ACMA, MUSIC, and CBF algorithms for applications to PCL systems. Narrow band PCL systems that use FM signals are studied using both uncorrelated-white and colored noise. Comparison is based on separation performance, error expected values, variances and success rate. If the DOA estimation error for both objects is less than or equal to 1.5°, it is called *success*.

5. Assumptions

The source signal is an FM signal at a 100 MHz carrier frequency with a 75 KHz bandwidth. This means that source signal, and object signals are constant modulus signals i.e., for all t, $|\mathrm{s}_i(\mathrm{t})| = c$.

Possible object signals are constant signals with Doppler shifts. There is no range information. The object signals correspond to Swerling cases 1, 3 and 5 in radar theory [8: 373-440]. This is applicable only for constant object signals with Doppler shift and not for random signals.

A passive receiver of linear array antennas, which has 16 uniformly spaced isotropic elements, is simulated. Figure 1 shows the antenna pattern. The array is assumed to be calibrated so that the array response vector $\mathbf{a}(\theta)$ is a known function. The ACMA algorithm requires that the array manifold satisfy the uniqueness condition, i.e., every collection of p vectors on the manifold is linearly independent [4].

Initial object directions and coordinates are fixed. Objects fly at constant speed within a single coherent processing interval (CPI).

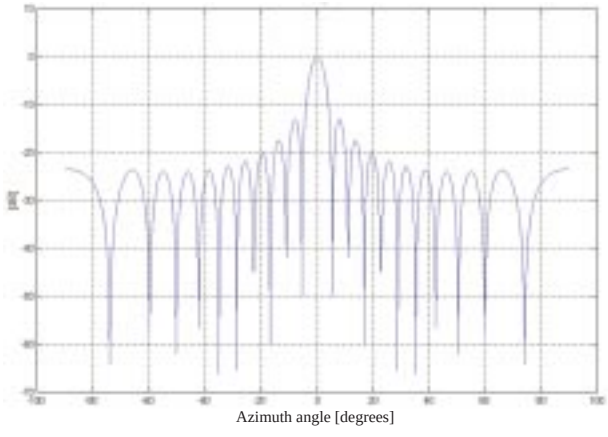

Figure 1. Antenna pattern.

6. Model Exploration

6.1. Signal Modeling

Typically, the real part of an FM signal can be depicted as

$$Re\{s_i(t)\} = \cos(w_c t + w_s t) \tag{1}$$

Another way to write this equation is

$$Re\{s_i(t)\} = \cos(w_c t + \gamma(t)) \tag{2}$$

Since we are modeling a narrow band system, we can add object Doppler to the signal above as

$$Re\{s_i(t)\} = \cos(w_c t + \gamma(t) + d(t)) \tag{3}$$

According to the assumptions in this study, the terms $\gamma(t)$ will be constant and $d(t)$ will represent a constant phase shift for each snapshot within a single CPI. The received object signals and source signal are simulated with SNR value related to a unit-variance noise signal. This may be used for a uniform linear array with isotropic elements. SNR means the ratio of the signal power to the noise power for each signal, at each of the antenna elements, and each of the time snapshots. The amplitude of the signal is, therefore, $10^{(SNR/20)}$. Then equation (3) becomes

$$Re\{s_i(t)\} = 10^{\frac{SNR}{20}} \cos(w_c t + \gamma(t) + d(t)) \tag{4}$$

This is the real part of the signal. We have a complex envelope, thus equation (4) should be rewritten as

$$s_i(t) = 10^{\frac{SNR}{20}} e^{j(w_c t + \gamma(t) + d(t))} \tag{5}$$

6.2. Signal Data Matrix

Data model [8] can be written as

$$\mathbf{x}(t) = \mathbf{ABs}(t) + \mathbf{n}(t) \tag{6}$$

where

$\mathbf{x}(t) = [x_1(t), \ldots .., x_p(t)]^T$ is a p x 1 vector of received signals at time t.

$\mathbf{A} = \mathbf{A}(\theta) = [\mathbf{a}(\theta_1), \ldots .., \mathbf{a}(\theta_q)]$, where $\mathbf{a}(\theta)$ is the array response vector for a signal from a direction θ, and $\theta = [\theta_1, \ldots \ldots, \theta_q]$ is the DOA vector of the signals.

$\mathbf{B} = \mathrm{diag}(\beta)$ is the channel gain matrix, with parameters $\beta = [\beta_1, \ldots .. \beta_q]^T$, where $\beta_i \in \mathrm{R}^+$ is the amplitude of the i-th signal as received by the array,

$\mathbf{s}(t) = [\mathrm{s}_1(t), \ldots .,\mathrm{s}_q(t)]^T$ is a q x 1 vector of signals at time t,

$\mathbf{n}(t)$ is the p x 1 additive noise vector, which is assumed spatially and temporally white Gaussian distributed with covariance matrix $\nu\mathbf{I}$, where $\nu = \sigma^2$ is the noise variance. Noise standard deviation for the real part and for the imaginary part is set to $\sqrt{1/2}$. Therefore, the total power of the noise equals one.

Unequal signal powers are absorbed in the gain matrix $\mathbf{B}$. Phase offsets of the signals after demodulation are part of the vector $\mathbf{s}_i$. Thus it can be written $\mathrm{s}_i(\mathrm{t}) = \mathrm{e}_i^{j\varphi(t)}$, where $\varphi_i(\mathrm{t})$ includes the unknown phase modulation for signal i, and the Doppler shift due to object movement. $\varphi_i(\mathrm{t}) = [\varphi_1(\mathrm{t}), \ldots, \varphi_q(\mathrm{t})]^T$ is defined as the phase vector for all objects at time t.

There will be N samples available.

$$\mathbf{X} = [\mathbf{x}(1), \ldots, \mathbf{x}(N)]^T$$

Thus, $\mathbf{X}$ is the data matrix with different channels as different rows and different snapshots as different columns.

7. DOA Estimation

Once we acquire the signal data matrix **X,** we can apply signal-processing techniques to estimate the DOA.

7.1. DOA Estimation with MUSIC and CBF

To estimate the DOA using MUSIC and CBF, the following steps are followed:

- Estimation of the signal correlation matrix,
- Estimation of the output DOA spectrum,
- Estimation of DOA.

7.1.1. Estimation of the signal correlation matrix

The correlation matrix estimate is based on the maximum likelihood (ML) estimate. This is, basically, the calculation of the maximum-likelihood correlation-matrix estimate of the received signals from different channels. The signal correlation matrix can be calculated using

$$\mathbf{R_{xx}} = \frac{1}{N}\mathbf{X}\mathbf{X}^H \tag{7}$$

where

$\mathbf{R}_{xx}$ is the sample correlation matrix,

N is the number of snapshots.

7.1.2. Estimation of Output DOA spectrum

The DOA-spectrum output is a quadratic measure of the presence of source and object signals in different directions. The output can be either a power spectrum or a pseudo spectrum. MUSIC and CBF estimate DOA using the pseudo or power spectrum. Both algorithms are heavily based on a sample correlation matrix, which introduces additional errors to DOA estimation. CBF estimates the power spectrum (Figure 2) using the sample correlation matrix, MUSIC estimates pseudo spectrum (Figure 3) using eigen-value-decomposition of the sample correlation matrix. MUSIC is an eigenanalysis-based algorithm using "noise subspace" eigenvectors. As the number of dominant eigenvalues increases due to non-zero bandwidth and power leakage, the subspace loses dimension [9]. This introduces additional errors to DOA estimation. The problem gets worse when a powerful signal at the antenna is present. The descriptions, detailed explanation and comparison of the MUSIC and CBF algorithms can be found in Johnson and Dudgeon [10].

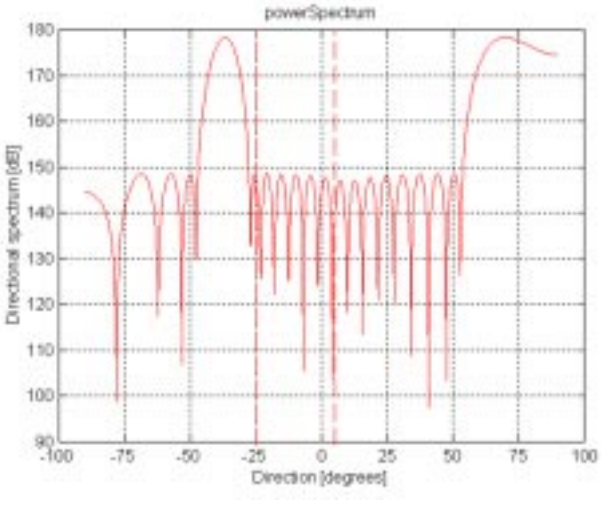

Figure 2. CBF power spectrum.

7.1.3. Estimation of the DOA

Peaks of the DOA spectrum give DOA estimates.

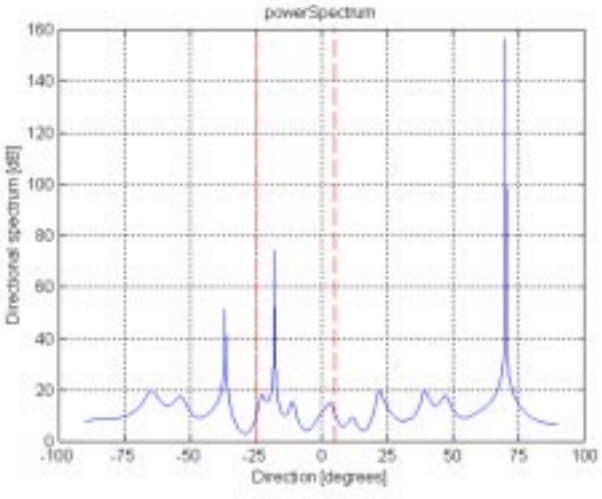

Figure 3. MUSIC pseudo stpectrum.

7.2. DOA Estimation with ACMA

ACMA, blindly, separates object signals from each other using constant modulus (CM) factorization, and estimates a corresponding array response. A simple projection of this array response estimate onto actual array response gives the decoupled DOA estimate. Since we have object signal estimates, we may further the process and extract Doppler or other information. Thus, we have single Doppler information that belongs to single DOA information. This saves the time that we need to associate Doppler and DOA values, and prevents data loss during this association process. To estimate the DOA using ACMA as in Figure 4, the following steps are followed:

- Blind source separation,
- Estimation of the array response for each signal,
- Estimation of the DOA for each signal.

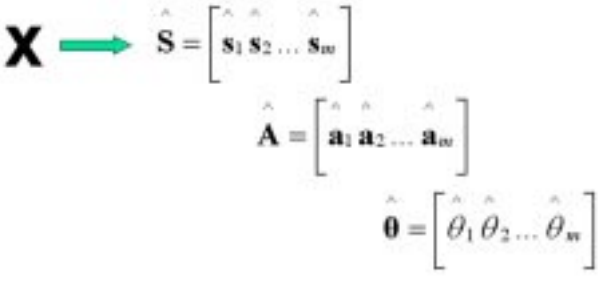

Figure 4. DOA estimation process with ACMA.

7.2.1. Blind Source Separation

The main advantage of ACMA is signal separation. We directly have DOA histories and signal estimates (Figure 5) for those histories, and we know that each set belongs to a single object. We, therefore, do not require any complicated filtering or association processes. We may use some additional process to detect false estimated data, especially when object SNR are low. Van Der Veen and Paulraj discuss the details of the algorithm [11].

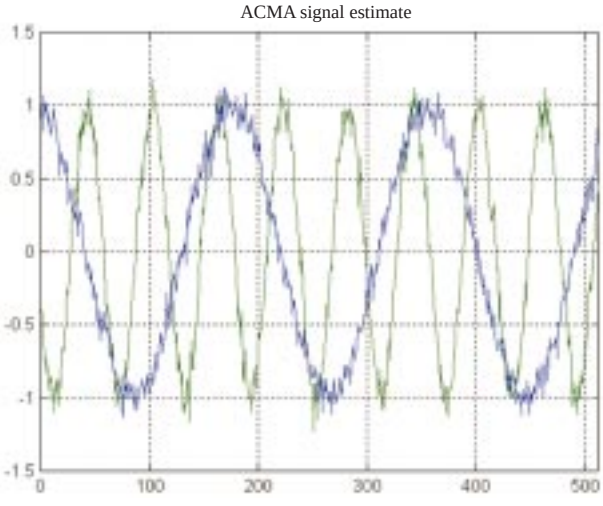

Figure 5. Estimated signals out of an ACMA separation process.

In summary, the signal estimate matrix is obtained as follows:

1. Estimate row ($\mathbf{X}$):
   a. Compute singular value decomposition, SVD($\mathbf{X}$): $\mathbf{X} = \mathbf{USV}$
   b. Estimate d = rank($\mathbf{X}$) from $\mathbf{S}$: the number of signals
   c. Redefine $\mathbf{V}$ as first d rows of $\mathbf{V}$
2. Estimate ker(Ps), which summarizes all CM conditions:
   a. Construct $\mathbf{Ps}$: $(n\text{-}1)\times d^2$ from $\mathbf{V}$
   b. Compute SVD($\mathbf{Ps}$): $\mathbf{Ps} = \mathbf{U}_p\mathbf{S}_p\mathbf{V}_p$
   c. Estimate δ = dim ker($\mathbf{Ps}$) from $\mathbf{S}_p$: the number of CM signals
   d. $[\mathbf{y}_1, \ldots, \mathbf{y}_\delta]$ = last δ columns of $\mathbf{V}_p$.
3. Solve the simultaneous diagonalization problem,
4. Recover the signals. [11:9]

Since finding the minimizers of the distance function [11:7] is involved, iteration is needed.

7.2.2. Estimation of the array response for each signal

ACMA provides the estimate of the array response for each separated signal. Figure 6 shows array response estimates for objects sitting at -25° and 5°.

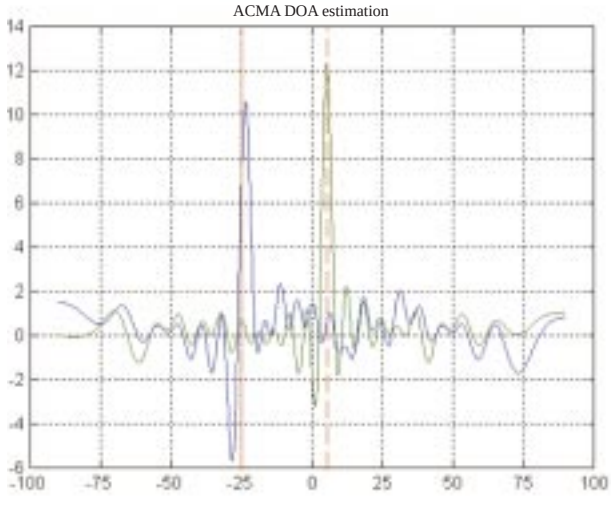

Figure 6. Estimated array responses out of ACMA process.

7.2.3. Estimation of the DOA for each signal

The ML estimate of one-dimensional projection of each array response estimate onto the known array response gives the estimation of the DOA for the corresponding signal estimate [12]. The ML estimate of the projection is defined as

$$\hat{\theta}_i = \arg\max_{\theta} \frac{\left|\hat{a}_i * a(\theta)\right|}{\|a(\theta)\|} \tag{8}$$

7.3. Differential ACMA

In this paper, we introduce differential ACMA. Since ACMA blindly separates constant modulus signals and estimates corresponding array responses, it is possible to identify the signal estimate that belongs to a direct source signal using a magnitude of the subsequent estimated array response. We can further remove the set that belongs to a direct source signal and recombine other estimated signals belonging to objects and their array response estimates together. This process gives us a direct-source-signal-free estimate of antenna output. Now we can reapply ACMA to this antenna output estimate. Figure 7 presents the schematic representation of a differential ACMA process.

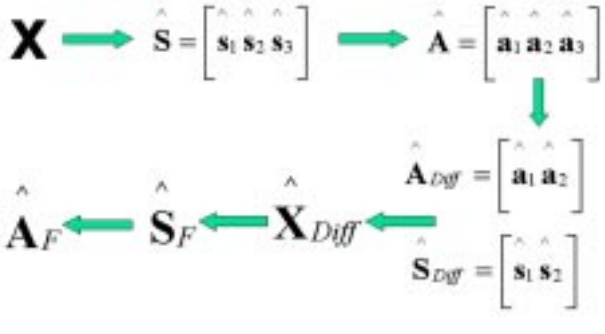

Figure 7. DOA estimation process with differential ACMA.

Figure 8 shows estimated signals out of differential ACMA. Examining Figures 5 and 8 together, we observe that differential ACMA gives us a better phase estimate.

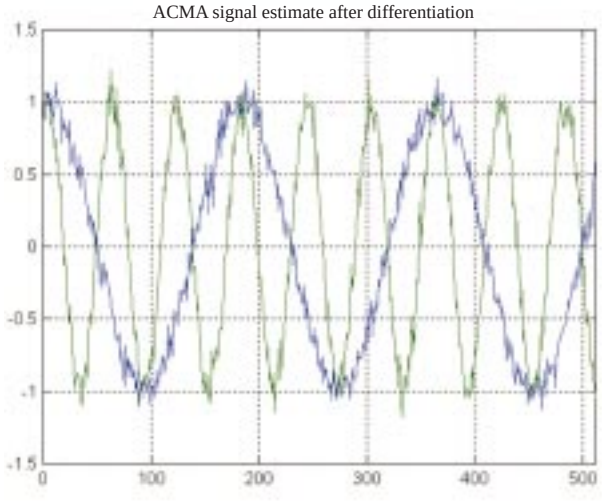

Figure 8. Estimated signals out of a differential ACMA separation process.

8. Designed Tests

We designed four different tests in order to evaluate the performance of the three DOA algorithms. All tests are based on 400 trials. Simulations are carried out in MATLAB®. It is known that as the number of samples increases the sample covariance matrix gets closer to the true covariance matrix. Thus, errors due to differences between sample covariance matrix and true covariance matrix are decreased. On the other hand, for radar applications, small CPIs are encouraged. Thus, we carried out two sets of simulations; in the first set we used $N = 512$ samples, and in the second set we used $N = 100$ samples for less CPI.

8.1. Test Number (1): Directional Test

This test, it is the goal to see the directional performance of the algorithms. Antenna element spacing is 0.5λ, which is the optimum value for maximum look angle. Thus, we have optimal evaluations of the algorithms for directional coverage. There is only one object. The test is performed for all directions from -90° to 90° using 1° increments. The SNR values are set to -10, 0 and 10 dB.

8.2. Test Number (2) : Separation Test

This test seeks to examine the separation performance of the algorithms. Element spacing bigger than 0.5λ introduces grating lobes to the antenna pattern, and this reduces directional coverage. Our interest of region lies within 30° for this and following tests. Thus, we set antenna element spacing is 0.65λ to have the advantage of having better antenna gain within 30° of boresite, and low mutual coupling. There are two objects. One of the objects is fixed at 5°, and the other object's position will be varied from -10° to 10° using 1° increments relative to the fixed one. The SNR values used are [-10 –10], [-10 10], and [10 10] dB.

8.3. Test Number (3): Suppression Test

This test seeks to examine the separation performance of the algorithms under the suppression of strong non-constant modulus signals. Antenna element spacing is 0.65λ. There are two objects. One of the objects is fixed at 5°, and the other object's position will be varied from -30° to 10° using 0.25-degree increments relative to the fixed one. The SNR values are [0 0], [5 5], and [10 10] dB. There is a source representing galactic noise at -50° (SNR = -15 dBm). There is an interfering signal (random-like color noise) at -15° (SNR = 50 dB). There is another interfering signal (random) at 60° (SNR = 15 dB).

8.4. Test Number (4) : Direct Source Signal Test

This test seeks to examine the separation performance of the algorithms under the suppression of strong non-constant modulus signals and direct source constant modulus signal. Antenna element spacing is 0.65λ. There are two objects. One of the objects is fixed at 5°, and the other objects' position will be changed from -30° to 10° using 0.25° increments relative to the fixed one. The SNR values are [0 0], [5 5], and [10 10] dB. There is a source representing galactic noise at -50° (SNR = -15 dBm). There is an interfering signal (random like color noise) at -18° (SNR = 50 dB). There is a direct source signal (constant modulus) at 70° (SNR = 170 dB).

9. Results and Analysis

For test 1, we present two sets of figures, expected errors and variances. For tests 2, 3 and 4, there will be an additional set presenting estimated DOA. In these figures, we should see two straight lines corresponding to each object DOA track. However, there are deviations, which belong to the false estimated DOA values. Figures that show expected errors, and variances for tests 2, 3 and 4 have three lines. At the first line, we present results for the moving object, and at the second line we present results for the fixed-one. There is a third line, which shows separation performances for algorithms. Figures for tests 2, 3 and 4 are only for 10 dB SNR values.

ACMA shows the best performance, and CBF shows the worst. MUSIC offers some good features, but ACMA has several robust features. For MUSIC and CBF algorithms, when the signals get closer, DOA estimation is degraded. ACMA can provide reasonable DOA estimates even though we have SNR values as low as –10 dB.

Comparing the results based on 512 samples to the results based on 100 samples, we see that there is a decrease in the performance of MUSIC and CBF algorithms as the number of samples available decreases due to the increased difference between the sample covariance matrix and true covariance matrix. For high noise levels, closely spaced signals or small N, the vectors out of the CM factorization step in ACMA can be used as initial starting points in Gerchberg iteration [11], which effectively searches for the minima of distance function. Since these starting points are accurate, a few iterations are adequate to obtain independent signals. The performance of the ACMA is therefore less affected. In severely ill-conditioned cases, more iteration is helpful.

9.1. Test 1: Directional Test

We show here that all three algorithms behave almost the same. There is no significant performance difference between them; however, Figure 10 shows better variance values for ACMA. For all three algorithms, the directional coverage increases as the SNR increases.

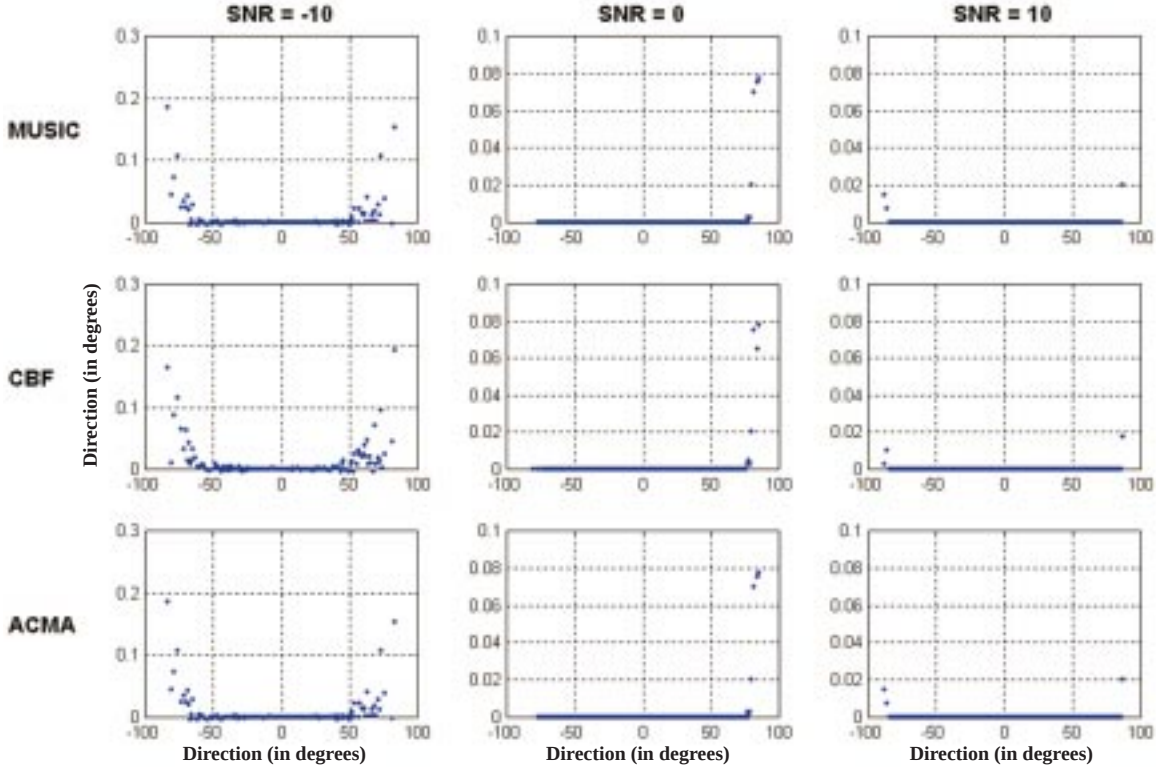

Figure 9. Expected errors.

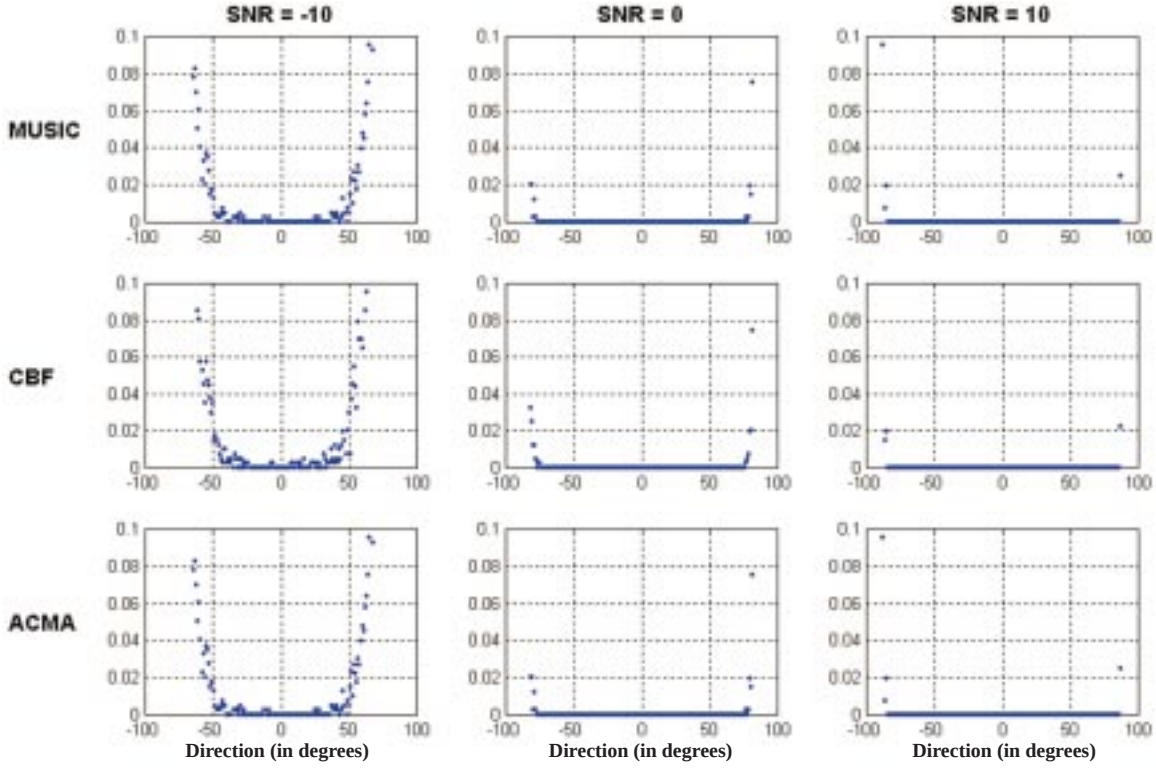

Figure 10. Variances.

9.2. Test 2: Separation Test

MUSIC estimates are unbiased when objects are not very close to each other. If objects are closer than 3°, MUSIC cannot separate the object signals anymore and produces one estimate when SNR equals to –10 dB for both objects. The DOA errors within this 3° region can be as high as 80° with variances up to 600°-squared. As SNR increases, separation performance improves. Figure 11 shows that MUSIC can separate objects as close as 1° when SNR equals 10 dB for both objects. Variances also get smaller as SNR increases.

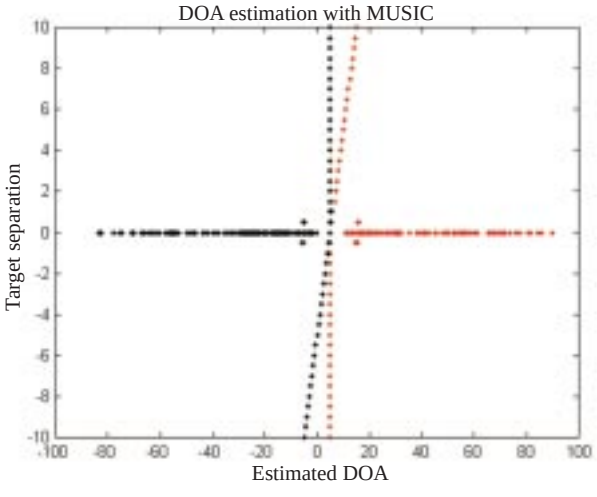

Figure 11. Estimated DOAs with MUSIC, SNR = [10, 10] dB.

CBF has the lowest variances, but it is the algorithm that behaves worst all circumstances. Figure 12 clearly shows that separation is a concern. CBF cannot separate objects closer than 6°. If objects have different SNR values like [-10, 10] dB, CBF cannot separate them within 8°. The signal with less power is swamped by the signal with high power.

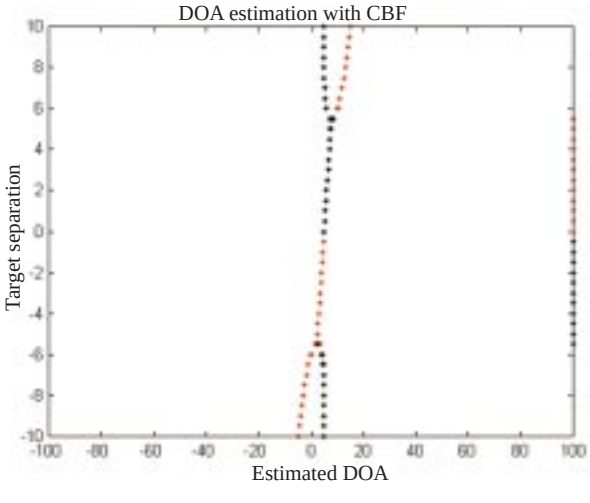

Figure 12. Estimated DOAs with CBF, SNR = [10, 10] dB.

Since ACMA provides signal separation, DOA estimation is decoupled and done separately for each signal. Thus, we expect better separation characteristics for ACMA compared with the other two algorithms.

Results show that ACMA can separate objects not closer than 2° even if the objects' SNR is –10 dB. Figure 13 shows that ACMA can separate objects as close as 0.25° when SNR equals 10 dB for both objects.

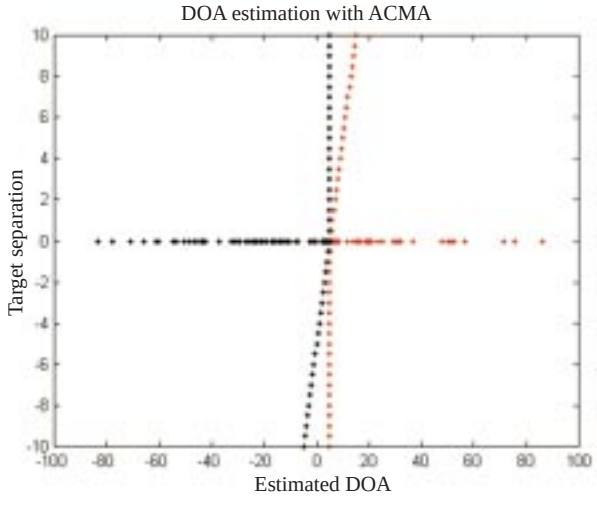

Figure 13. Estimated DOAs with ACMA, SNR = [10, 10] dB.

9.3. Test 3: Suppression Test

The results of this test, as seen in Figure 14, show that CBF cannot estimate the DOA of objects accurately, even the SNR values as high as 10 dB.

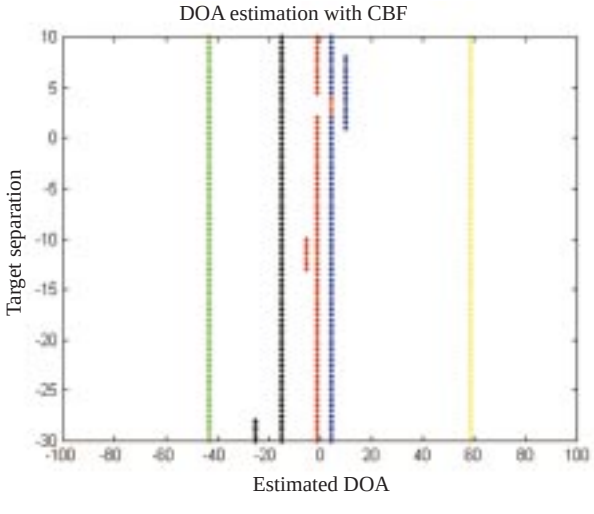

Figure 14. Estimated DOAs with CBF, SNR = [10, 10] dB.

Figure 15 shows estimated DOA data with MUSIC for five signals: three interfering signals, and two object signals. Examining those figures, we clearly see that to discover the most accurate estimates belonging to two objects, we should have some extra information, like Doppler history. This requires additional processing and time. In order to have accurate estimates belonging to objects, a non-linear filter, possibly a Kalman filter, should be applied. This is a complicated process. When objects SNR are small, this filtering process becomes much more complicated, and data loss is possible. Even if we have accurate estimates from a non-linear process, we should still associate those estimated DOAs and Doppler

processing results in order to have two separate sets of object information. In this research, no non-linear processing has been done. Therefore, the statistical evaluation of MUSIC and CBF at tests 3 and 4 was not studied. Examining estimated DOA data plots, we observe that the presence of a high-SNR colored-noise source adversely affects results of the MUSIC algorithm.

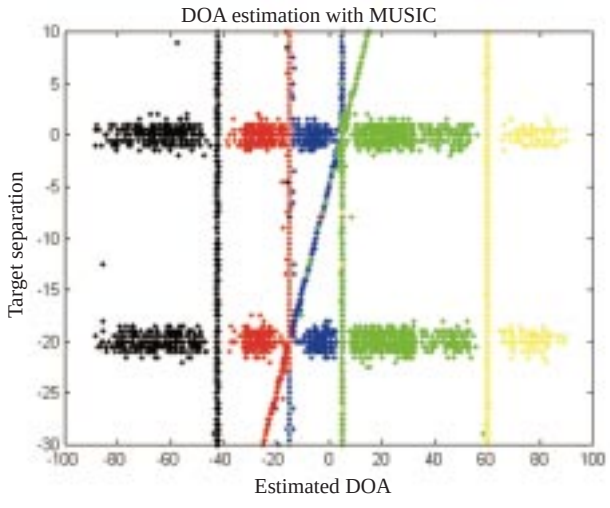

Figure 15. Estimated DOAs with MUSIC, SNR = [10, 10] dB.

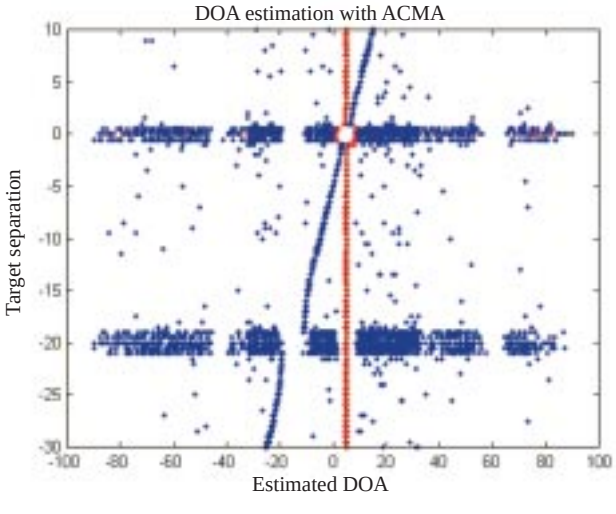

Figure 16. Estimated DOAs with ACMA, SNR = [10, 10] dB.

The case in this test shall be categorized as an ill-conditioned case. Thus, we use 30 Gechenberg iterations. We also study no iteration cases. Results without iterations show low error levels; however, they are not stable and have high variances due to the colored-noise source. As expected, iteration helps to remove the effect of the colored-noise source signal, but it introduces small bearing error.

Examining the results, we observe that the separation performance of ACMA is degraded in comparison to the white-noise case. Iteration is another cause for this corruption. In a high-colored noise environment, ACMA can separate objects no closer than 2.5° when object's SNRs are 0 dB. In Figures 16, 17, and 18 we further observe that ACMA can separate objects if they are no closer than 1° to each other when the objects' SNRs are 10 dB. It is possible to have large errors and high variances, as the object

gets closer to the 50 dB colored-noise source signal. Corruption begins as the object gets closer than 3°, regardless of object SNR levels. At low SNR levels, high-colored noise source causes high variances. In Figures 17 and 18 we observe that there are problems around -20° caused by the interfering random signal.

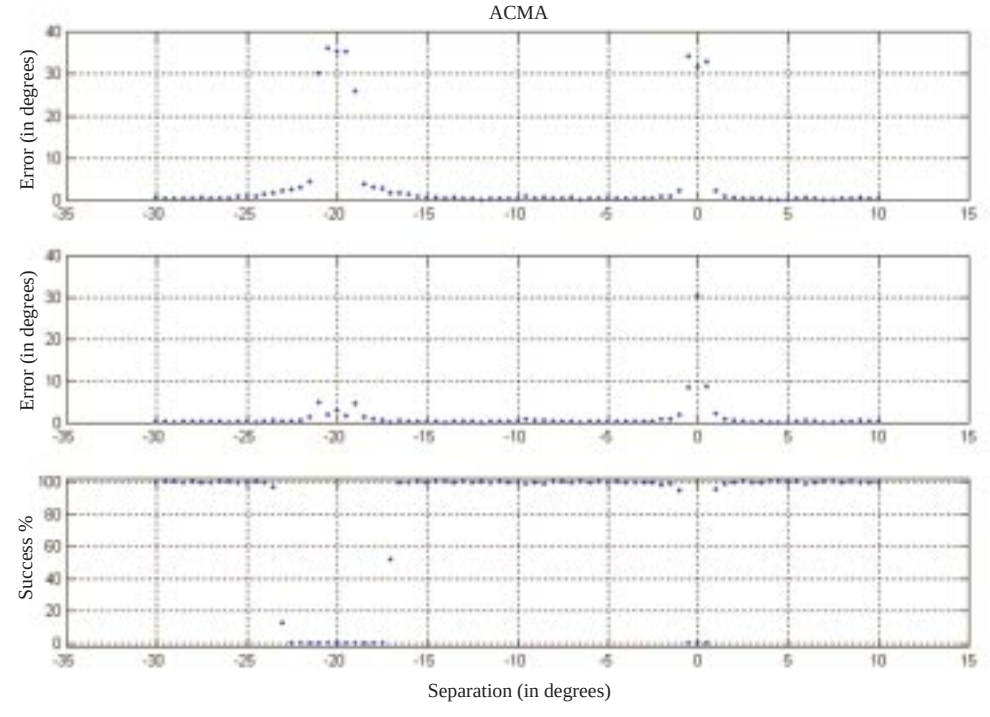

Figure 17. Expected errors, SNR = [10, 10] dB.

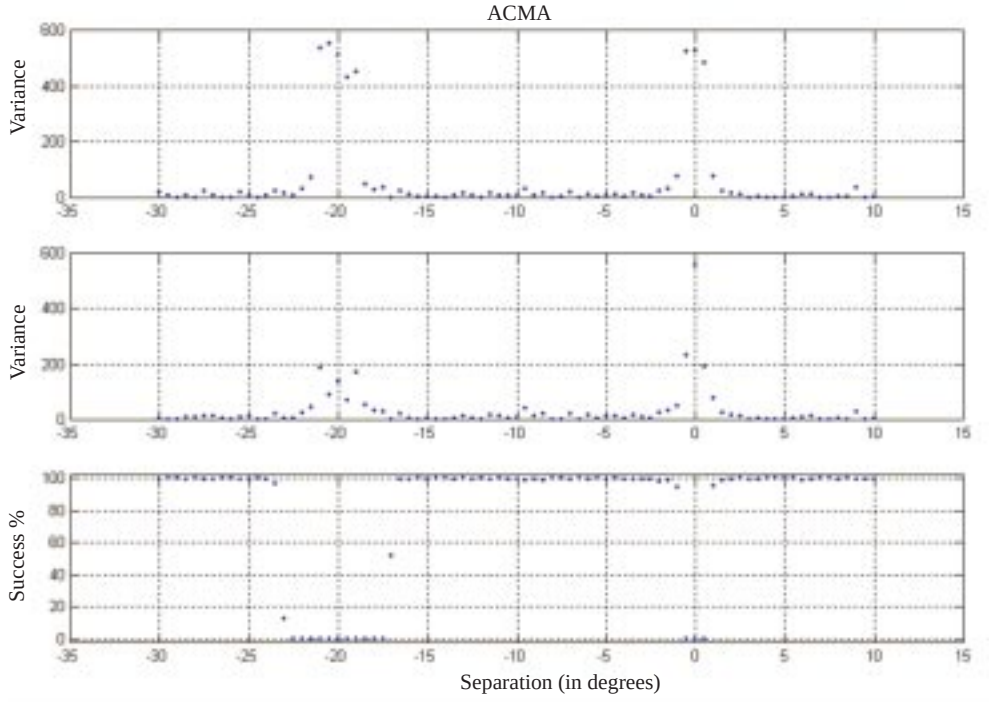

Figure 18. Variances, SNR = [10, 10] dB.

9.4. Test 4: Direct Source Signal Test

In Figure 20 we observe that CBF cannot estimate the DOA of objects accurately, even if object SNRs are as high as 10 dB. MUSIC behaved even worse than it did in test 3. In Figure 19, it is observed that the presence of a direct source signal adversely affects the results of the MUSIC algorithm. For the 10 dB SNR level, there is almost no chance to extract object DOA from MUSIC estimations.

As seen in Figures 23, 24 and 25 differential ACMA continues to give us DOA estimates even if we have a strong direct source signal at the antenna with a high-colored noise source signal.

In this test, we use 30 Gechenberg iterations for both ACMA estimations. We also study the no iteration case. Results without iterations show high error levels, and they are not stable and have high variances. Iteration helps to remove the effect of the colored-noise source signal, but it introduces a small bearing error. Differentiation helps to remove the effect of direct source signal. Differentiation also helps to remove some effects of the colored-noise source signal.

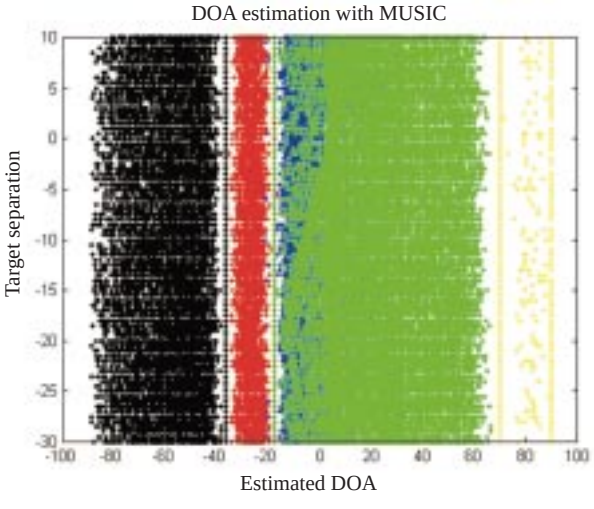

Figure 19. Estimated DOAs with MUSIC, SNR = [10, 10].

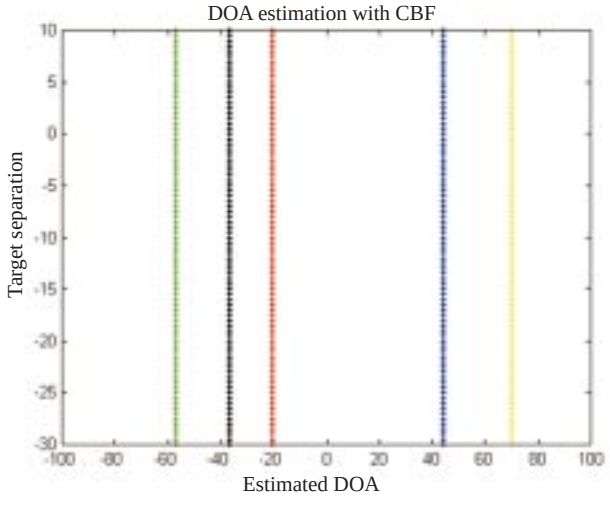

Figure 20. Estimated DOAs with CBF, SNR = [10, 10].

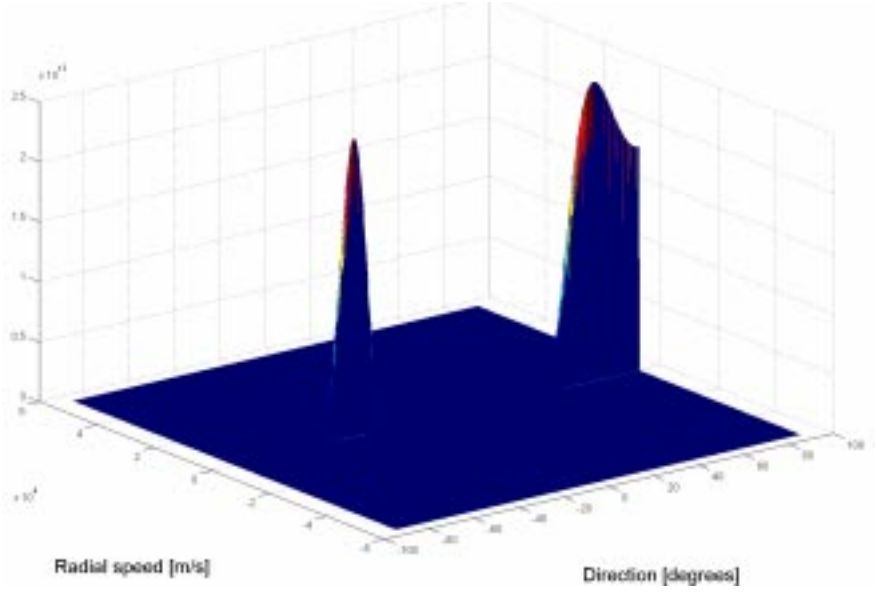

Figure 21. Adaptive total finite response filter. (no differentiation).
Filter is applied to the antenna output after beamforming. No differentiation is used. The antenna output includes two objects at 5 and –25° (10 dB SNR), a direct source signal at 70° (170 dB SNR), and an interfering signal at –18° (50 dB SNR).

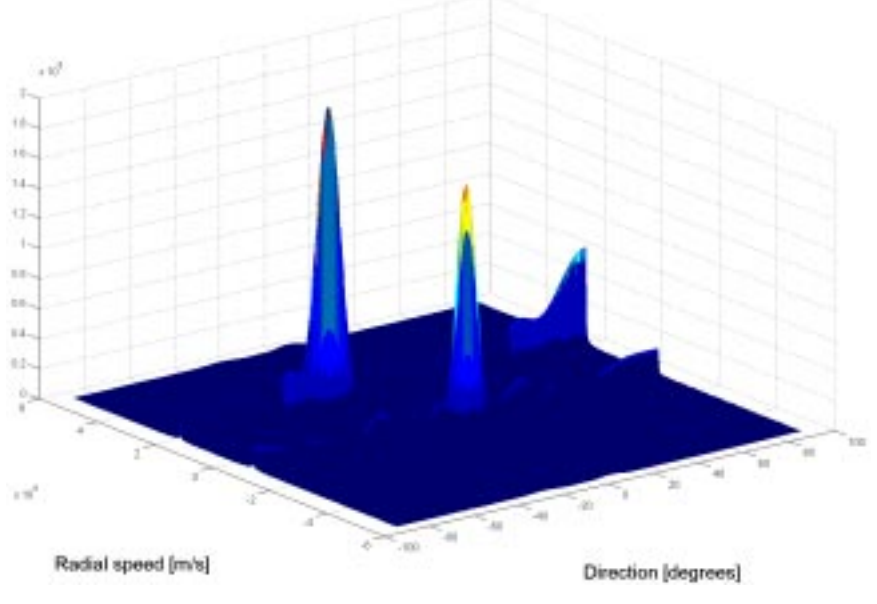

Figure 22. Adaptive total finite response filter (with differentiation).
Differentiation is used. Filter is applied to the antenna output estimate after differentiation.

Figure 21 shows the adaptive total finite time filter result. The filter was applied to the original antenna output. Since the power of the direct source signal and the interfering signal are higher than the power of the two objects, the objects' signals are filtered out. On the other hand, the two objects' signals are clearly seen in Figure 22.

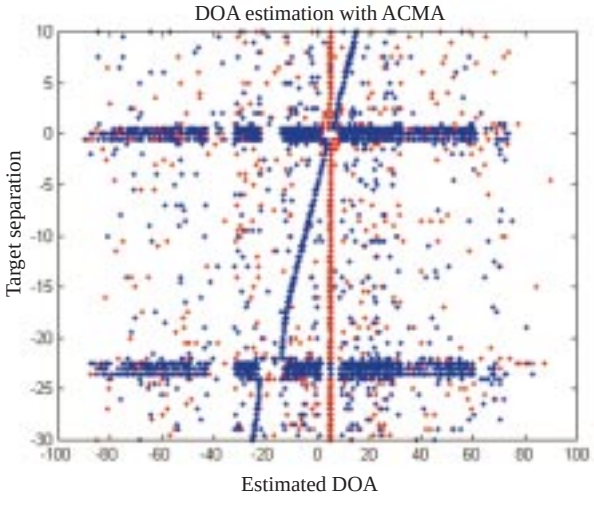

Figure 23. Estimated DOAs with ACMA, SNR = [10, 10].

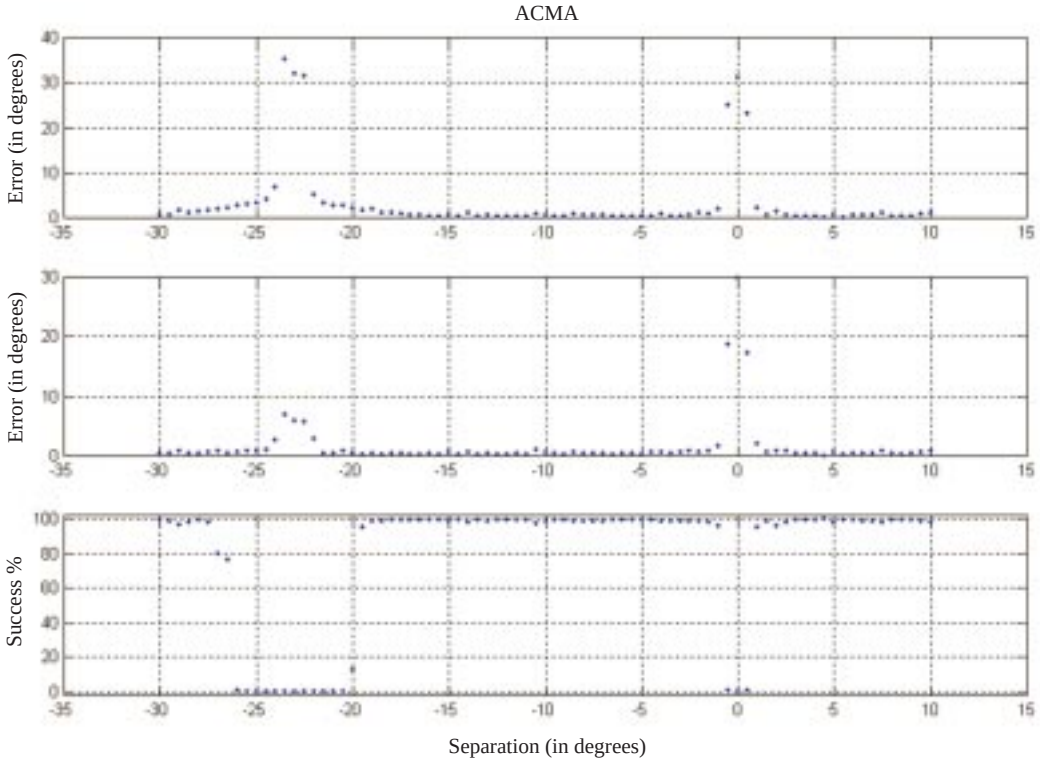

Figure 24. Expected errors, SNR = [10, 10].

10. Conclusion

The results and analyses presented here support the idea that the constant modulus information, where available, is an important addition to DOA estimation. ACMA is a still relatively young. It offers many simple solutions to noise and separation-related problems. The basic advantage of ACMA is that it provides a signal estimate. A reliable signal estimate permits further information extraction and reduces problems in data association.

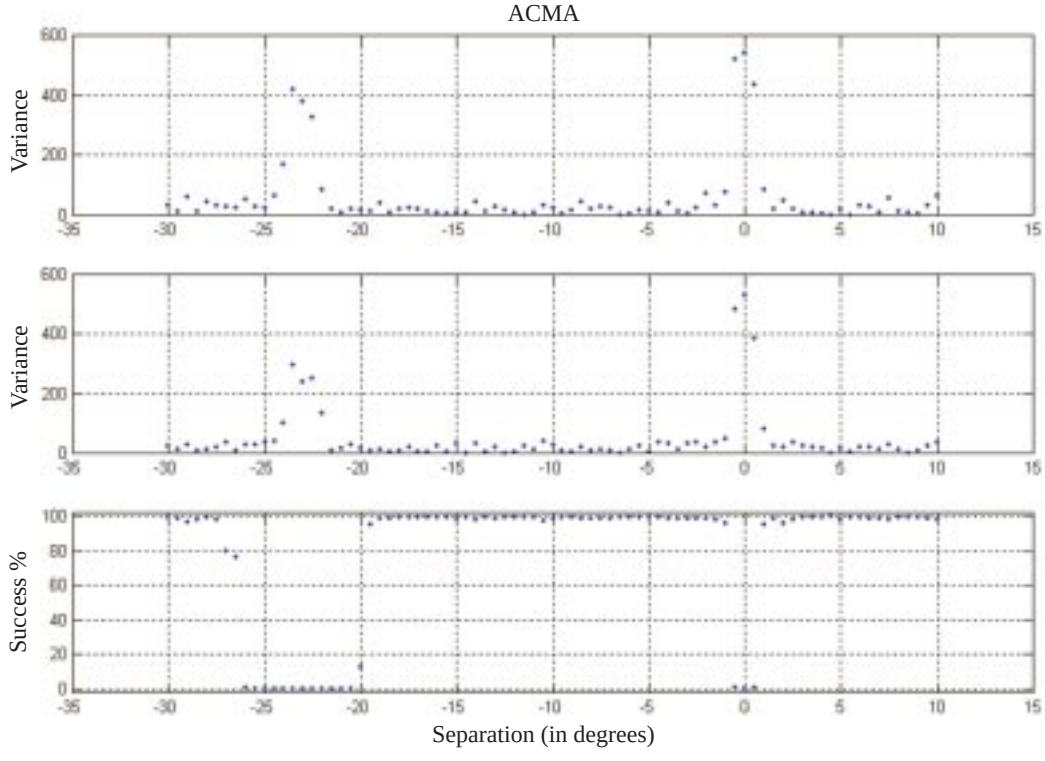

Figure 25. Variances, SNR = [10, 10].

We estimate that the separation performance of ACMA is better than that of the other two algorithms. It can provide accurate DOA estimates even if a direct source signal or additional high-colored noise source signals at the antenna are present. In addition, differential ACMA, which allows the digital removal of the direct signal component from the output of a sensor array in a simple way, is introduced.

It is clear that ACMA can provide improved performance over the CBF and MUSIC algorithms. At low SNR levels (-10 dB), ACMA provides much more accurate estimates and yields reasonable separation performance even in the presence of challenging signals.

The results and analyses presented here are situation dependent. Further analysis for other situations is useful. In this work, only one iteration technique is used for ACMA. Other iteration techniques should be examined. In addition, non-linear processes were not studied; e.g., statistical evaluations for MUSIC and CBF are not presented. A comparison based on available statistical evaluations of the MUSIC and CBF algorithms to ACMA would be useful.

Finally, the results and analysis are based on Matlab® simulations. Due to difficulties obtaining real data, we chose to use a simulation. Verification of the results with real data should provide a better understanding of the topic.

Acknowledgments

I am grateful to numerous individuals who contributed to this project. First, I wish to thank Bob Ogrodnik, AFRL/SNRD, Nicholas Willis, Technology Service Corp, and Dr. Aaron Lanterman, GTRI, who have given lectures at seminar, and provided suggestions and insights through e-mails and videoconferences. I am also very thankful to Dr. Aaron Lanterman for his support from his electronic library of PCL. I also appreciate

Darek Maksimiuk's efforts to help me with Matlab simulations.

References

[1] Howland, P.E. "Target Tracking Using Television-Based Bistatic Radar," *IEEE Proceedings, Radar, Sonar Navigation,* 146-3: 166-174 (June 1999).

[2] Griffiths, H.D. and Long, B.A. "Television-based Bistatic Radar," IEEE Proceedings, Vol. F-133, No. 7, pp. 649-657, December 1986.

[3] Baniak, J. "Silent Sentry, Passive Surveillance." Article. http://www.dtic.mil/ndia/jaws/sentry.pdf. 31 July 2001.

[4] Van Der Veen, A.J. "Blind Source Separation Based on Combined Direction Finding and Constant Modulus Properties." Proceedings IEEE, SP Workshop on Statistical Signal and Array Processing, pp. 380-383, September 1998.

[5] Scharf, L.L. Statistical Signal Processing: Detection, Estimation and Time Series Analysis. New York: Addison-Wesley Publishing Company, Inc., 1991.

[6] Leshem, A. "Maximum Likelihood Separation of Phase Modulated Signals." Proceedings IEEE ICASSP, 1999.

[7] Trump, T. and Ottersten, B. "Estimation of Nominal Direction of Arrival and Angular Spread Using an Array of Sensors," Royal Institute of Technology, Signal Processing, Vol. 50, pp. 1-24, April 1996.

[8] Leshem, A. and Van Der Veen, A.J. "Bounds and algorithm for direction finding of phase modulated signals." in Proceedings IEEE workshop on Statistical Signal Array Processing, Sept. 1998.

[9] Sorelius, J., Moses, R.L., Soderstorm, T. and Swindlehurst, A.L. "Effects of Non-Zero Bandwidth on Direction of Arrival Estimators in Array Signal Processing." IEEE Proc. Radar, Sonar, & Navig., December, 1998.

[10] Johson, D.H. and Dudgeon, D. E. Array Signal Processing: Concepts and Techniques. New Jersey: PTR Prentice-Hall, Inc., 1993.

[11] Van Der Veen, A.J. and Paulraj, A. "An Analytical Constant Modulus Algorithm." IEEE Transactions on Signal Processing, Vol. 44, No. 5, pp. 1-19, May 1996.

[12] Leshem, A. and Van Der Veen, A.J. "Direction of Arrival Estimation for Constant Modulus Signals." IEEE Transactions on Signal Processing, Vol. 47, No.11, pp. 3125-3129, Nov 1999.